LBNL-45524
Preprint

ERNEST ORLANDO LAWRENCE
BERKELEY NATIONAL LABORATORY

Osmotic Second Virial Coefficient, Intrinsic Viscosity and Molecular Simulation for Star and Linear Polystyrenes

Alberto Striolo, John M. Prausnitz,
and Alberto Bertucco

Chemical Sciences Division

April 2000

Submitted to
Polymer

REFERENCE COPY
Does Not
Circulate
Bldg. 50 Library - Ref.
Lawrence Berkeley National Laboratory
Copy 1
LBNL-45524

DISCLAIMER

This document was prepared as an account of work sponsored by the United States Government. While this document is believed to contain correct information, neither the United States Government nor any agency thereof, nor The Regents of the University of California, nor any of their employees, makes any warranty, express or implied, or assumes any legal responsibility for the accuracy, completeness, or usefulness of any information, apparatus, product, or process disclosed, or represents that its use would not infringe privately owned rights. Reference herein to any specific commercial product, process, or service by its trade name, trademark, manufacturer, or otherwise, does not necessarily constitute or imply its endorsement, recommendation, or favoring by the United States Government or any agency thereof, or The Regents of the University of California. The views and opinions of authors expressed herein do not necessarily state or reflect those of the United States Government or any agency thereof, or The Regents of the University of California.

Ernest Orlando Lawrence Berkeley National Laboratory
is an equal opportunity employer.

DISCLAIMER

This document was prepared as an account of work sponsored by the United States Government. While this document is believed to contain correct information, neither the United States Government nor any agency thereof, nor the Regents of the University of California, nor any of their employees, makes any warranty, express or implied, or assumes any legal responsibility for the accuracy, completeness, or usefulness of any information, apparatus, product, or process disclosed, or represents that its use would not infringe privately owned rights. Reference herein to any specific commercial product, process, or service by its trade name, trademark, manufacturer, or otherwise, does not necessarily constitute or imply its endorsement, recommendation, or favoring by the United States Government or any agency thereof, or the Regents of the University of California. The views and opinions of authors expressed herein do not necessarily state or reflect those of the United States Government or any agency thereof or the Regents of the University of California.

LBNL-45524

Osmotic Second Virial Coefficient, Intrinsic Viscosity and Molecular Simulation for Star and Linear Polystyrenes

Alberto Striolo and John M. Prausnitz*

Department of Chemical Engineering
University of California, Berkeley
and
Chemical Sciences Division
Ernest Orlando Lawrence Berkeley National Laboratory
University of California
Berkeley, California 94720

and

Alberto Bertucco

Istituto di Impianti Chimici
Università di Padova
Via Marzolo 9
I-35131 Padova, Italy

April 2000

*To whom correspondence should be addressed.

This work was supported by the Director, Office of Science, Office of Basic Energy Sciences, Chemical Sciences Division, of the U.S. Department of Energy under Contract No. DE-AC03-76SF00098.

recycled paper

LBNL-45524

Osmotic Second Virial Coefficient, Intrinsic Viscosity and Molecular Simulation for Star and Linear Polystyrenes

Alberto Striolo and John M. Prausnitz
Department of Chemical Engineering
University of California
and
Chemical Sciences Division
Lawrence Berkeley National Laboratory
University of California
Berkeley, CA 94720, U.S.A.
and
Alberto Bertucco
Istituto di Impianti Chimici
Università di Padova, Via Marzolo 9, I-35131 Padova, Italy

April 2000

This work was supported by the Director, Office of Science, Office of Basic Energy Sciences, Chemical Sciences Division of the U.S. Department of Energy under Contract Number DE-AC03-76SF00098.

Abstract

Experimental osmotic second virial coefficients are reported for polystyrene in toluene (good solvent), cyclohexane (theta solvent) and methylcyclohexane (poor solvent) in the temperature range 10 to 60°C. At good solvent conditions, the osmotic second virial coefficient for a branched polymer is lower than that for a corresponding linear homolog. Branching lowers the theta temperatures for a given solvent-polymer system. The theta temperature for 8-arm star polystyrene in methylcyclohexane is 29±3°C.

Intrinsic viscosity for polystyrene in cyclohexane and methylcyclohexane has been measured over a wide temperature range. A coil-globule transition has been observed for 8-arm star polystyrene in methylcyclohexane at temperatures close to the theta temperature.

Standard Monte Carlo simulation calculations have been used to study the dilute-solution properties of star polymers with 3, 4, 5, and 6 arms. Solvent conditions were represented by square-well attractive potentials between non-bonded polymer segments. Radii of gyration, asphericity, center-to-end distance, and arm radii of gyration have been obtained as a function of molecular weight. Second virial coefficients have been computed for 6-arm star polymers of two molecular weights. Molecular-simulation results show a depression of the theta temperature for star polymers compared to those of linear homologs, in agreement with experiment.

Key words: Osmotic Second Virial Coefficient, Intrinsic Viscosity, Monte Carlo Simulation, Potential of Mean Force, Radius of Gyration

Introduction

Regular star polymers are branched structures where equi-sized linear arms emanate from a central core. Because the core is usually small in size it does not significantly affect any thermodynamic property. Star polymers with up to 450 arms with desired chemical and molecular weight asymmetries can be synthesized [1]-[3]. Possible

industrial applications of star polymers have been discussed (see [4]-[7] and references therein).

Star polystyrene has been used to produce porous membranes with well-defined size distribution and well-defined positions of the pores [8].

For concentrated solutions (up to 0.5 solvent weight fraction), the effect of polymer structure upon solvent sorption is very small [9], [10], but branching seems to increase solubility.

Osmotic second virial coefficients and mean-square radii of gyration in dilute solutions have been measured [11]-[18]. In good solvents, the osmotic second virial coefficient is smaller for branched polymers than that for the homolog linear polymers (see, for example, [19] and [20]). Some studies report that the theta temperature for star polystyrene in cyclohexane is higher than that for the corresponding linear polystyrene [21]. Others report that branching lowers the theta temperature of a solvent-polymer system. For star-branched polymers of given molecular weight, deviations of the theta temperature from that for a linear polymer increase as the number of arms increases and as the arm molecular weight decreases [22], [23]. This and other experimental evidence [24]-[27] suggest that branching raises solubility.

The goal of this work is to advance our understanding concerning how polymer molecular architecture is related to thermodynamic properties.

Previous studies have supported a 'colloidal-nature' view of highly branched star polymers in dilute and semi-dilute solutions [28]-[30]. The experimental osmotic pressures could be interpreted in a colloid-like framework [28] using an approximate potential of mean force. Molecular simulation provides an alternate way to interpret the experimental results and to understand the microscopic basis of macroscopic properties.

On-lattice [31]-[33] and off-lattice [34]-[37] models of linear polymers have been used in simulation studies to compute radii of gyration and potentials of mean force for polymers in solution. However, there are few simulations for equilibrium properties of star polymers and most of them are based on lattice models. Primary interest was generally devoted to radius of gyration and to segment radial distribution function [38]-[44]. The potential of mean force between star polymers has been determined, but only at good-solvent conditions [45]-[47].

In this work, an off-lattice model is used to study molecular characteristics (size, shape, scaling exponents) and the potential of mean force for star polymers in dilute solution.

This paper is organized as follows:

Section A presents measured osmotic pressure.

Section B presents measured intrinsic viscosity.

Section C presents the Monte Carlo simulation method and results.

Section D compares results from computer simulation to our experimental data.

A. Experimental Osmotic Second Virial Coefficients

Osmotic pressures were measured with a membrane osmometer, model 231, from Jupiter Instrument Co., Jupiter, Florida (USA). The temperature was kept constant at ±0.2°C over a 12-hour period with an electric-resistance heater. Measurements were made for solutions of linear polystyrene in toluene and cyclohexane, and for 8-arm star polystyrene in toluene, cyclohexane and methylcyclohexane. Polymers were kept under vacuum two or three days before an osmotic-pressure measurement to ensure removal of low-molecular-weight impurities. Table 1 shows polymer characteristics and Table 2 shows solvent characteristics. Solvents were used as received. Cellulose acetate membranes were supplied by Jupiter Instrument Co., the molecular-weight-cut-off was 20,000 g/mole.

The osmotic pressure, Π, of a polymer solution can be expressed by a virial expansion (see, for example, Tombs and Peacoke, [48]):

$$\frac{\Pi}{R \cdot T} = \frac{1}{M_n} \cdot c + B_{22} \cdot c^2 + B_{222} \cdot c^3 + \ldots \quad , \tag{1}$$

where R, M_n, B_{22}, B_{222} and c are respectively, the gas constant, the polymer's number-average molecular weight [49], second and third virial coefficients and polymer mass concentration. At low polymer concentration, terms of order higher than second can be neglected, and Equation 1 reduces to:

$$\frac{\Pi}{R \cdot T} \cdot \frac{1}{c} = \frac{1}{M_n} + B_{22} \cdot c \quad . \tag{2}$$

The results reported for B_{22} and M_n are obtained from fitting the experimental data to Equation 2.

Results and Discussion

Table 3 shows experimental molecular weights and osmotic second virial coefficients. When polydyspersity is taken into account, the molecular weight is generally comparable to that obtained from the supplier, except for linear polystyrene of high molecular weight (LPSHM) in cyclohexane, where the molecular weight is too high to be determined by osmometry.

Figure 1 shows experimental osmotic second virial coefficients for star polystyrene of low molecular weight (SPSLM), star polystyrene of high molecular weight (SPSHM), linear polystyrene of low molecular weight (LPSLM), and linear polystyrene of high molecular weight (LPSHM) in toluene. No significant temperature dependence was observed for star polymers in the temperature range considered. B_{22} does not show strong dependence upon polymer architecture. However, in agreement with other experimental observations [12], [20], [50], B_{22} for star polymers is slightly smaller than those for linear polymers of the same molecular weight. It is likely that the difference follows from the relative dimensions of the two polymers; star polymers have a radius of gyration smaller than that of linear polymers [51]. The difference in osmotic second virial coefficient for star and for linear polymers of the same molecular weight is expected to decrease with rising arm molecular weight for star polymers with the same number of arms. Figure 1 shows this trend for the polymers studied here.

Figure 2 shows osmotic second virial coefficients for LPSLM and SPSLM in cyclohexane at temperatures close to the theta temperature for the linear polymer (34.5°C [49]). The osmotic second virial coefficient for LPSLM shows a strong dependence on temperature and a theta temperature very close to the literature value. On the other hand, B_{22} for SPSLM is positive and nearly independent of temperature, indicating that the theta temperature for the branched structure is lower than that for the linear structure. The lowering of theta temperature caused by branching, more pronounced for low-molecular-weight arms [25], [52]-[53], may follow from the high segment density close to the core [53] or from 'end-chain' effects [11]. Molecular simulation may clarify these

experimental observations, as well as the 'arm stretching' observed at low distances from the core [54].

Figure 3 shows osmotic second virial coefficients for SPSLM in methylcyclohexane. Extrapolating to the temperature where B_{22} equals zero, the theta temperature is 29±3°C. By contrast, for linear polystyrene in methylcyclohexane, the theta temperature lies between 60 and 70°C [55]; our results show that, for this polymer-solvent system, one branching point alone is able to lower the theta temperature by about 35°C.

Typical experimental results in Figure 4 show osmotic pressure as a function of concentration for two linear polystyrenes, one with low and the other with relatively high molecular weight (LPSLM, LPSHM) in toluene. From these plots it is possible to obtain rough estimates of the third osmotic virial coefficients, reported in Table 4, as required to fit the experimental data. The third osmotic virial coefficients B_{222} have been obtained fitting the experimental data with Equation 1 when M_n and B_{22} are the experimental values reported in Table 3.

B Intrinsic viscosity

Intrinsic viscosity was measured by a conventional capillary viscometer of the Ubbelohde type. A water bath was used to maintain the temperature at ±0.2°C. The intrinsic viscosity of LPSLM in cyclohexane and that of SPSLM in cyclohexane and in methylcyclohexane were measured over a wide temperature range.

The intrinsic viscosity, [η], for sufficiently long polymer chains [56] is a function of the radius of gyration according to:

$$[\eta] = \frac{K \cdot \langle R_g^{\,2} \rangle^{3/2}}{M_v} \quad , \tag{3}$$

where K, $\langle R_g^2 \rangle$, M_v are, respectively, Flory's viscosity factor [57], average radius of gyration squared and polymer viscosity-average molecular weight [49]. K is essentially constant for a given polymer architecture [58]. This coefficient is subject to an incremental increase with rising branching density [59]. A linear polymer contracts to a compact form when the solvent quality decreases, as happens, for example, when

lowering the temperature [60]-[64]; at very low temperatures, polymer may aggregate. The coil-globule transition occurs near the theta temperature.

In the poor-solvent regime [η] is a unique function of the polymer radius of gyration, irrespective of polymer's architecture [65].

From experimental [η] it is possible to calculate the polymer's dimension as a function of temperature (see for example [62]-[64], [66], [67]).

The expansion factor α is defined by

$$\alpha = \left(\frac{\langle R_g^{\,2} \rangle}{\langle R_g^{\,2} \rangle_0} \right)^{1/2} \tag{4}$$

where subscript 0 indicates the unperturbed dimensions; α characterizes the extent to which polymer-solvent interactions expand or contract the chain dimensions over their unperturbed values. The expansion factor is unity at theta conditions [56]. It is also possible to define the 'viscosity' expansion factor [62] as

$$\alpha_\eta = \left(\frac{[\eta]}{[\eta]_0} \right)^{1/3} . \tag{5}$$

In what follows, the expansion factor is assumed equal to the viscosity expansion factor. Renormalization-group theory [60] suggests that the expansion factor near the theta temperature obeys the scaling law

$$\alpha \propto \left(N \cdot \tau^2 \right)^k , \tag{6}$$

where N is the degree of polymerization and τ is the reduced temperature defined as

$$\tau = \frac{\vartheta - T}{T} . \tag{7}$$

Here ϑ is the theta temperature [62]. In Equation 6, exponent k is a parameter that attains different values for temperatures higher or lower than ϑ. The same ideas are here applied to both linear and star polymers close to their theta states.

An independent measurement of the theta temperature can be obtained from plotting intrinsic viscosity versus temperature [56], [62] at temperatures near the coil-globule transition temperature.

Figure 5 shows the intrinsic viscosity as a function of temperature. While for LPSLM in cyclohexane a coil-globule transition is evident in the temperature range investigated (see, also, Sun et al., [62] and [63]), no transition is observed for SPSLM in the same solvent. However, a coil-globule transition was observed for SPSLM in methylcyclohexane. These measurements suggest that the theta temperature for the star polystyrene in cyclohexane is lower than that for the linear counterpart. In Figure 6 the expansion factor is plotted as a function of the reduced temperature multiplied by the square root of the molecular weight for LPSLM in cyclohexane and for SPSLM in methylcyclohexane. The reduced temperature was computed assuming a theta temperature of 34.5°C for LPSLM in cyclohexane and 30.5°C for SPSLM in methylcyclohexane. Because the plot appears to follow a universal law for the description of the collapse near the theta temperature, 30.5°C is probably close to the theta temperature for SPSLM in methylcyclohexane. This experimental observation provides independent evidence for the theta temperature 29±3°C for SPSLM in methylcyclohexane obtained from osmotic-pressure measurements.

C. Molecular Simulation

A polymeric chain is represented by a sequence of freely-jointed hard spheres of diameter σ. A star polymer is here represented by 3, 4, 5, or 6 linear chains of the same molecular weight connected to the core. The solvent is considered to be a continuum. The interactions present in the system are represented by hard-sphere repulsion (two segments are not allowed to overlap) and by square-well attraction between non-bonded segments. The square-well potential between non-bonded segments is:

$$\phi(d) = \begin{cases} \infty & d < \sigma \\ \varepsilon & \sigma \le d \le 1.5 \cdot \sigma \end{cases}, \tag{8}$$

where σ, ε, and d represent respectively the segment diameter, the well depth and the center-to-center distance between two segments. Well depth ε ranges from zero to –0.50 k_BT. k_BT is Boltzmann's constant and T is the absolute temperature. Equation 8 allows us to calculate temperature-dependent properties of dilute polymer solutions.

Dynamic Monte Carlo techniques, such as the efficient reptation algorithm [68], [69], are not suitable to generate equilibrium configurations of branched structures because the branching point does not permit deletion of one polymer segment from one end of the chain and attachment to the other end. The Pivot algorithm is here used [70], [71]. The Metropolis algorithm is used for acceptance criteria. The system is equilibrated with 1.5 million trial moves. In the production phase, 1000 independent conformations [71] are stored and used to compute geometric characteristics of star polymers.

The ensemble average radius of gyration squared $<R_g^2>$ has been computed according to

$$< R_g^{\ 2} >=< \frac{1}{n} \cdot \sum_{i=1}^{n} \left[(x_i - x_{cm})^2 + (y_i - y_{cm})^2 + (z_i - z_{cm})^2 \right] > \ , \tag{9}$$

where n is the total number of segments in the polymer, x_i, y_i, and z_i are the coordinates of the ith segment and x_{cm}, y_{cm}, and z_{cm} are those of the polymer molecule's center of mass.

The average shape of polymers is of importance for a variety of phenomena, especially for dilute-solution hydrodynamics. The shape of a polymer coil in dilute solution, when averaged over a long period of time, is spherical. However, numerous studies have reported the instantaneous asymmetry of equilibrium linear chains in dilute solutions (see, for example, Theodorou et al., [72]). It is likely that star polymers with many arms are more symmetric than linear polymers. For each simulated polymer, the square of the main components of the radius of gyration, λ_1, λ_2, λ_3, have been computed according to Rudnick and Gaspari, [73]. These components are used in the definition of asphericity, A:

$$A = \frac{\sum_{q>p}^{3} (\lambda_q - \lambda_p)^2}{2 \cdot \left(\sum_{p=1}^{3} \lambda_p \right)^2} \ . \tag{10}$$

In Equation 10, λ_p and λ_q are the squares of the main components of the radius of gyration. Asphericity A is an indication of the symmetry of a polymer molecule; it has a lower bound equal to zero for spherical molecules, while it is unity for rod-like molecules

[73]-[76]. The sample average asphericity, <A>, has here been computed as a function of the number of arms, arm molecular weight, and solvent quality

The potential of mean force is computed following the algorithm proposed by Hall and coworkers [36], [37] and slightly modified by Lue and Prausnitz [77]. The potential of mean force, W (r), as a function of the distance between the centers of mass of the polymers, r, is obtained by:

$$\frac{W(r)}{k_B \cdot T} = -\ln \frac{\sum_{l=1}^{C} U_l(r)}{C} \quad , \tag{11}$$

where C is the total number of polymer pairs used at each distance and U_l (r) is the statistical weight of each polymer pair at given separation r. This statistical weight is obtained by:

$$U_l(r) = \exp^{\frac{-\Phi_l(r)}{k_B \cdot T}} \quad , \tag{12}$$

where Φ_l (r) is the potential between two interacting polymers. This quantity is equal to infinity if at least one segment of one polymer overlaps with a segment of the other polymer. If there are no overlaps, it is equal to the number of segment pairs belonging to the two interacting polymers distant less than 1.5 times the segment diameter σ, multiplied by the well depth. 1,000,000 polymer pairs were used at each separation r. The results reported are the average of at least three different runs.

Results

Table 5 presents the ensemble-average radius of gyration squared, $<R_g^2>$; asphericity, <A>; arm radius of gyration squared $<R_{arm}^2>$; and center-to-end distance squared, $<D_{CTE}^2>$, computed for the star polymers at different solvent conditions.

Figure 7 shows the radius of gyration squared for a model 6-arm star polymer as a function of the total number of segments at different well depths. A scaling law

$$\left\langle R_g^{\,2} \right\rangle = \gamma \cdot n^{\nu} \quad , \tag{13}$$

can be observed at every well depth. Here n is the total number of segments in the polymer molecule, and γ and ν are constants. For linear polymers, the theta condition can be defined as that where the scaling exponent ν equals unity. Interpolating the scaling

factors, the conditions at which the scaling exponent equals unity for 3-, 4-, 5-, and 6-arm star polymers correspond to –0.34±0.02 k_BT, -0.35±0.02 k_BT, -0.355±0.015 k_BT, and –0.355±0.015 k_BT respectively. These results show that the theta temperature for a star polymer decreases with rising number of arms. However, given the accuracy of these calculations, no appreciable difference can be observed between 5- and 6-arm star polymers.

The ratio of the squared radius of gyration of a star polymer, $\langle R_g^2 \rangle_{star}$, to the squared radius of gyration of a linear polymer of the same molecular weight, $\langle R_g^2 \rangle_{linear}$, for Gaussian chains [20], [78] is given by [79]:

$$\frac{\langle R_g^2 \rangle_{star}}{\langle R_g^2 \rangle_{linear}} = \frac{3 \cdot f - 2}{f^2} \tag{14}$$

where f is the number of arms in the star polymer. Figure 8 shows the radii of gyration for the homolog linear polymers obtained from Equation 14 using the radii of gyration for star polymers with different number of arms, for a well depth of –0.30 k_BT. Data for linear polymers [36] are also shown for comparison. Good agreement is found between radii of gyration predicted from Equation 14 and those simulated for linear polymers [36]. Well depth equal to –0.30 k_BT is near theta conditions for both linear and star polymers.

The instantaneous conformation is asymmetric. At good solvent conditions, values of <A> generally agree with results reported by Bishop and coworkers [80]. Our results show that <A> for a 3-arm star polymer decreases with falling solvent quality, but for 4-, 5-, and 6-arm star polymers, <A> shows a maximum with falling solvent quality. Jagodzinski [81] reported renormalization-group-theory calculations for the asphericity of star polymers of infinite molecular weight. Table 6 shows the estimates obtained for random-walk star polymers. Our results are generally lower than those estimates; however, insufficient data were obtained to extrapolate to infinite molecular weight the asphericity of star polymers. Generally, for a star polymer with a given number of arms, <A> increases with rising arm-molecular weight. As expected, <A> decreases with rising number of arms for a star polymer of given molecular weight [81]. Therefore, a

star polymer looks more and more like a sphere with rising number of arms and with decreasing arm length [80].

Figure 9 shows the sample-average arm radius of gyration squared as a function of the number of segments in the arm, for a well depth of –0.40 k_BT. For a fixed number of segments, the arm radius of gyration increases with rising number of arms, especially for low-molecular-weight arms, probably because of the high segment density around the core that is expected to increase with rising number of arms. This result agrees with results from Ganazzoli and coworkers [54], [82] who calculated the distances between segments in a star polymer in the excluded-volume regime, and with results from Daoud and Cotton [38]. However, our results show that 'arm-stretching' is more pronounced at poor solvent conditions.

Figure 10 shows the potential of mean force as a function of the distance between the centers of mass of the polymers for athermal star polymers with different number of arms and comparable molecular weight. The difference in potential of mean force between linear and star polymers in good solvents increases with rising number of arms. In particular, at good solvent conditions, the second osmotic virial coefficient for star polymers of given molecular weight decreases with rising number of arms [45] due to the declining polymer radius of gyration. For 6-arm star polymer, the potential of mean force is infinity at separations between the centers of mass less than half the radius of gyration. Therefore, it is not possible for two 6-arm star polymers to penetrate into each other.

Figure 11 shows the potential of mean force computed for 6-arm star polymer, 17 segments per arm, as a function of the distance between centers of mass, under different solvent conditions. From the potential of mean force, we compute the second virial coefficient according to:

$$B_{22}^{1} = 2 \cdot \pi \cdot \int_{0}^{\infty} r^{2} \cdot \left(1 - \exp\left[-\frac{W(r)}{k_B \cdot T}\right]\right) \cdot dr \quad . \tag{15}$$

In this form, B^{1}_{22} is expressed in volume units. B_{22} and B^{1}_{22} are related by:

$$B_{22} = \frac{B_{22}^{1} \cdot N_A}{M_n^{\,2}} \quad , \tag{16}$$

where N_A is Avogadro's number. Table 7 shows the osmotic second virial coefficients computed for 6-arm star polymers of two different molecular weights under different

solvent conditions. Theta conditions are those where the osmotic second virial coefficient is zero. Interpolating the results, the theta states for 6-arm star polymer of 103 and of 205 total segments correspond to -0.35 ± 0.01 k_BT and to -0.35 ± 0.015 k_BT respectively. The difference in molecular weight between the two 6-arm star polymers is not enough to change the theta temperature, given the uncertainties of our calculations. The well depth corresponding to the theta temperature is the same as that where the scaling exponent in Equation 13 equals unity.

D. Discussion

Our calculations give a difference in theta temperature of 0.03 ± 0.02 k_BT between linear [36] and 6-arm star polymers. For SPSLM in methylcyclohexane, the theta temperature is 29±3°C. For the linear homolog, our simulation results predict a theta temperature of about 60±15°C in rough agreement with the theta temperatures measured for linear polystyrene in methylcyclohexane [35].

Our simulation results show an increase in osmotic second virial coefficient with rising temperature for star polymers in agreement with our experimental results for SPSLM in methylcyclohexane.

Concluding remarks

The experimental osmotic second virial coefficients here reported confirm that branching lowers the osmotic second virial coefficient for polystyrene in toluene, a good solvent. The 8-arm star polystyrene used in this work has a theta temperature in cyclohexane lower than that for linear polystyrene. The theta temperature for SPSLM in methylcyclohexane is 29±3°C.

Intrinsic viscosities for polystyrene in cyclohexane and in methylcyclohexane have been measured as a function of temperature. There is no evidence for a coil-globule transition for SPSLM in cyclohexane in the temperature range considered, suggesting a theta temperature lower than that of linear polystyrene in cyclohexane. However, evidence for a coil-globule transition has been observed for SPSLM in methylcyclohexane, suggesting a theta temperature for this system near 30°C.

Monte Carlo simulation results confirm a decrease in theta temperature caused by branching. The predicted decrease in theta temperature between linear and 6-arm star polymer of comparable molecular weight agrees with the experimental theta temperature for SPSLM in methylcyclohexane. Scaling exponents are obtained for star polymers with different number of arms at different solvent conditions. For 6-arm star polymers, a scaling exponent equal to unity is found for well depth $-0.355\pm0.015\ k_BT$. The asphericity of star polymers of fixed molecular weight decreases with rising number of arms; for fixed number of arms, asphericity increases with rising arm length. Arm radii of gyration squared show a stretching of the arm at low arm-molecular weight caused by the high segment density around the core; stretching increases with rising number of arms. Osmotic second virial coefficients for 6-arm star polymers of 103 and of 205 total segments are calculated at different solvent conditions. The well depth corresponding to the theta temperature is $-0.35\pm0.015\ k_BT$.

Acknowledgments

This work was supported by the Director, Office of Science, Office of Basic Energy Sciences Chemical Science Division of the U.S. Department of Energy under Contract Number DE-AC03-76SF00098. Some simulation calculations were performed on a CRAY T3E at the NERSC supercomputing facility, Berkeley, CA. A.S. thanks the Italian Ministry of University and Scientific and Technological Research (MURST) for financial support. The authors are grateful to Prof. S.J. Muller for use of her viscometer, to Nancy Liang and Shereen Sackmann for assistance in data acquisition, and to L. Lue, D. Bratko, C. Mio, N. Elvassore and R. Curtis for helpful discussions.

References

1. Hadjichristidis, N. J. Polym. Sci. A Polym. Chem. 1999; 37: 857.

2. Cloutet, E.; Fillaut, J.-L.; Astruc, D.; Gnanou, Y. Macromolecules 1998; 31: 6748.

3. Grest, G.S.; Fetters, L.J.; Huang, J.S.; Richter, D. In Prigogine, I.; Rice, S.A. Editors Advances in Chemical Physics 1996; vol. 94, p. 67.

4. Simms, J.A. Progress in Organic Coatings, 1993; 22: 367.

5. Gomez-Elvira, J.M.; Halary, J.L.; Monnerie, L.; Fetters, L.J. Macromolecules 1994; 27: 3370.

6. Feng, H.; Feng, Z.; Shen, L. Macromolecules 1994; 27: 7840.

7. Guo, A.; Liu, G.; Tao, J. Macromolecules 1996; 29: 2487.

8. Widawski, G.; Rawiso, M.; Francois, B. Nature 1994; 369: 387.

9. Mio, C.; Prausnitz, J.M. Polymer 1998; 39: 25.

10. Lieu, J.C.; Prausnitz, J.M.; Gauthier, M. Polymer 2000; 41: 219.

11. Okumoto, M.; Terao, K.; Nakamura, Y.; Norisuye, T.; Teramoto, A. Macromolecules 1997; 30: 7493.

12. Okumoto, M.; Nakamura, Y.; Norisuye, T.; Teramoto, A. Macromolecules 1998; 31: 1615.

13. Huber, K.; Burchard, W.; Fetters, L.J. Polymer 1987; 28: 1997.

14. Willner, L.; Jucknischke, O.; Richter, D.; Roovers, J.; Zhou, L.-L.; Toporowski, P.M.; Fetters, L.J.; Huang, J.S.; Lin, M.Y.; Hadjichristidis, N. Macromolecules 1994; 27: 3821.

15. Willner, L.; Jucknischke, O.; Richter, D.; P.M.; Fetters, L.J.; Huang, J.S.; Farago, B. Makromol. Chem., Macromol. Symp. 1992; 61: 122.

16. Roovers, J.; Toporowski, P.M.; Douglas, J. Macromolecules 1995; 28: 7064.

17. Boothroyd, A.T.; Squires, G.L.; Fetters, L.J.; Rennie, A.R.; Horton, J.C.; de Vallera, A.M.B.G. Macromolecules 1989; 22: 3130.

18. Boothroyd, A.T.; Fetters, L.J. Macromolecules 1991; 24: 5215.

19. Gauthier, M.; Chung, J.; Choi, L.; Nguyen, T.T. J. Phys. Chem. B, 1998; 102: 3138.

20. Douglas, J.F.; Roovers, J.; Freed, K.F. Macromolecules 1990; 23: 4168.

21. Dondos, A.; Panagopoulos, D. Polymer 1997; 38 (25): 6255.

22. Bauer, B.J.; Hadjichristidis, N.; Fetters, L.J.; Roovers, J.E.L. J. Am. Chem. Soc. 1980; 102 (7): 2410.

23. Roovers, J.E.L.; Bywater, S. Macromolecules 1974; 7 (4): 443.

24. Numasawa, N.; Okada, M. Polymer Journal 1999; 31 (1): 99.

25. Terao, K.; Okumoto, M.; Nakamura, Y.; Norisuye, T.; Teramoto, A. Macromolecules, 1998; 31: 6885.

26. Yokoyama, H.; Takano, A.; Okada, M.; Nose, T. Polymer 1991; 32 (17): 3218.

27. Cowie, J.M.G.; Horta, A.; Mcewen, I.J.; Prochazka, K. Polymer Bul. 1979; 1: 329.

28. Likos, C.N.; Lowen, H.; Watzlawek, M.; Abbas, B.; Juckischke, O.; Allgaier, J.; Richter, D. Physical Review Letters 1998; 80 (20): 4450.

29. Dozier, W.D.; Huang, J.S.; Fetters, L.J. Macromolecules 1991; 24: 2810.

30. Roovers, J.; Zhou, L.; Toporowski, P.M.; van der Zwan, M.; Iatrou, H.; Hadjichristidis, N. Macromolecules 1993; 26: 4324.

31. Bishop, M.; Saltiel, C.J. J. Chem. Phys. 1991; 95 (1): 606.

32. Yuan, X.F.; Masters, A.J. J. Chem. Phys. 1991; 94 (10): 6908.

33. Olaj, O.F.; Pelinka, K.H. Makromol. Chem. 1976; 177: 3413.

34. Grosberg, A.Y.; Khalatur, P.G.; Khokhlov, A.R. Makromol. Chem., Rapid Commun. 1982; 3: 709.

35. Huber, K.; Burchard, W.; Bantle, S.; Fetters, L.J. Polymer 1987; 28: 863.

36. Dautenhahn, J.; Hall, C.K. Macromolecules 1994; 27: 5399.

37. Yethiraj, A.; Honnell, K.G.; Hall, C.K. Macromolecules 1992; 25: 3979.

38. Daoud, M.; Cotton, J.P. J. Physique 1982; 43: 531.

39. Huber, K.; Burchard, W.; Bantle, S.; Fetters, L.J. Polymer 1987; 28: 1990.

40. Zifferer, G. Macromol. Theory Simul. 1997; 6: 805.

41. Mansfield, M. L.; Stockmayer, W. H. Macromolecules 1980; 13: 1713.

42. Whittington, S.G.; Lipson, J.E.G.; Wilkinson, M.K.; Gaunt, D.S. Macromolecules 1986; 19: 1241.

43. Freire, J.J.; Rey, A.; de la Torre, J.G. Macromolecules 1986; 19: 457.

44. Zang, L. Polym. J. 1996; 28 (6): 471.

45. Rubio, A.M.; Freire, J.J. Macromolecules 1996; 29: 6946.

46. Ohno, K.; Shida, K.; Kimura, M.; Kawazoe, Y. Macromolecules, 1996; 29: 2269.

47. Lue, L.; Kiselev, S.B. Submitted to Macromolecules, 1999.

48. Tombs, M.P.; Peacocke, A.R. The osmotic pressure of biological macromolecules, Claredont Press, Oxford, 1974.

49. Young, R.J.; Lovell, P.A. Introduction to polymers, 2nd ed., Chapman & Hall, London, 1991.

50. Candau, F.; Rempp, P.; Benoit, H. Macromolecules 1972; 5: 627.

51. Higo, Y.; Ueno, N.; Noda, I. Polym. J. 1983; 15 (5): 367.

52. Bruns, W.; Carl, W. Macromolecules 1991; 24: 209.

53. Ganazzoli, F.; Allegra, G. Macromolecules 1990; 23 (1): 262.

54. Forni, A.; Ganazzoli, F.; Vacatello, M. Macromolecules 1996; 29: 2994.

55. Elias, H.-G. in Brandrup, J.; Immergut, E.H.; Grulke, E.A. Editors Polymer Hanbook, 4th Ed., John Wiley & Sons, Inc., New York 1999.

56. Baysal, B.M.; Uyanik, N. Polymer 1992; 33 (22): 4798.

57. Fox, T.G.; Flory, P.J. J. Am. Chem. Soc. 1951; 73: 1904.

58. Roovers, J.; Hadjichristidis, N.; Fetters, L.J. Macromolecules 1983; 16: 214.

59. Yamakawa, H. Modern theory of polymer solutions, Harper & Row, Publishers, New York, 1971.

60. Bauer, D.R.; Ullman, R. Macromolecules 1980; 13: 392.

61. Swislow, G.; Sun, S.-T.; Nishio, I.; Tanaka, T. Psys. Review Letters 1980; 44 (12): 796.

62. Sun, S.F.; Fan, J. Polymer 1997; 38 (3): 563.

63. Sun, S.F.; Chou, C.-C.; Nash, R.A. J. Chem. Phys. 1990; 93 (10): 7508.

64. Sun, S.-T.; Nishio, I.; Swislow, G.; Tanaka, T. J. Chem. Phys. 1980; 73 (12): 5971.

65. Ganazzoli, F.; Forni, A. Macromolecules 1995; 28: 7950.

66. Vidakovic, P.; Rondelez, F. Macromolecules 1985; 18: 700.

67. Stockmayer, W.H.; Fixman, M. J. Polym. Sci. C 1963; 1: 137.

68. Frenkel, D.; Smit, B. Understanding Molecular Simulation, Academic Press, San Diego, 1996.

69. Allen, M.P.; Tildesley, D.J. Computer Simulation of Liquids, Oxford Science Publications, Claredon Press, Oxford, 1987.

70. Lal, M. Molecular Physics 1969; 17: 57.

71. Kremer, K.; Binder, K. Computer Physics Reports 1988; 7: 259.

72. Theodorou, D.N.; Suter, U.W. Macromolecules 1985; 18: 1206.

73. Rudnick, J.; Gaspari, G. Science 1987; 237: 384.

74. Minato, T.; Hatano, A. Macromolecules 1981; 14: 1035.

75. Solc, K. J. Chem. Phys. 1971; 55 (1): 335.

76. Wei, G.; Eichinger, B.E. J. Chem. Phys. 1990; 93 (2): 1430.

77. Lue, L.; Prausnitz, J.M. Macromolecules 1997; 30 (21): 6650.

78. Ganazzoli, F.; Fontelos, M.A.; Allegra, G. Polymer 1993; 34 (12): 2615.

79. Zimm, B.H.; Stockmayer, W.H. J. Chem. Phys. 1949; 17 (12): 1301.

80. Bishop, M.; Smith, W. J. Chem. Phys. 1991; 95 (5): 3804.

81. Jagodzinski, O J. Phys. A: Math. Gen. 1994; 27: 1471.

82. Ganazzoli, F.; Fontelos, M.A.; Allegra, G. Polymer 1991; 32: 170.

Table 1 Polymer properties

Polymer	Acronym	Branch molecular weight (g/mole)	Total molecular weight (g/mole)	Polydispersity	Supplier
Linear polystyrene	LPSLM	-	73,000 [a]	1.04	Polymer Source, Inc.
Linear Polystyrene	LPSHM	-	343,700 [a]	1.05	Polymer Source, Inc.
8-arm star polystyrene	SPSLM	9,800	74,000	-	Polymer Source, Inc.
8-arm star polystyrene	SPSHM	46,700	391,000	-	Polymer Source, Inc.

[a] from size-exclusion chromatography.

Table 2 Solvent properties

Solvent	Purchased from	Lot number	Purity %
Toluene	Fisher Scientific	982728	99.8
Cyclohexane	Fisher Scientific	992006	99.7
Methylcyclohexane	Aldrich	LR08119KR	99

Table 3 Experimental osmotic second virial coefficients for polystyrene (PS), linear (L) and 8-arm star (S), of low (LM) or relatively high molecular weight(HM)

Polymer	Solvent	Temperature (°C)	M_n (10^{+3} g/mole)	B_{22} (10^{-7} l mole/g^2)
LPSLM	toluene	48.5	77 ± 2	3.95 ± 0.20
LPSHM	toluene	47.1	435 ± 80	3.95 ± 0.15
SPSLM	toluene	10.8	73 ± 1	3.6 ± 0.1
SPSLM	toluene	31.0	78 ± 1	3.90 ± 0.06
SPSLM	toluene	47.6	76.0 ± 0.5	3.22 ± 0.03
SPSLM	toluene	61.2	81 ± 3	3.3 ± 0.2
SPSHM	toluene	31.2	370 ± 50	3.5 ± 0.5
SPSHM	toluene	47.7	- *	3.57 ± 0.08
LPSLM	cyclohexane	23.3	55.0 ± 0.2	-2.87 ± 0.02
LPSLM	cyclohexane	27.8	73.0 ± 3.5	-1.10 ± 0.25
LPSLM	cyclohexane	33.8	77 ± 3	-0.12 ± 0.01
SPSLM	cyclohexane	23.3	59 ± 1	2.20 ± 0.25
SPSLM	cyclohexane	34.2	80 ± 5	1.5 ± 0.4
SPSLM	cyclohexane	43.1	80 ± 3	2.35 ± 0.60
SPSHM	cyclohexane	34.0	342 ± 9	0.79 ± 0.04
LPSLM	methylcyclohexane	45.7	- **	-2.8 ±0.1
SPSLM	methylcyclohexane	32.5	75 ± 3	0.18 ± 0.03
SPSLM	methylcyclohexane	42.0	77.5 ± 1.5	1.03 ± 0.02
SPSLM	methylcyclohexane	50.0	74 ± 1	1.3 ± 0.4

* molecular weight is too high to be determined by membrane osmometry.
** molecular weight cannot be measured in this poor solvent.

Table 4 Approximate experimental osmotic third virial coefficient for linear polystyrenes in toluene

Polymer	Temperature (°C)	B_{222} (10^{-9} mole l^2/g^3)
LPSLM	48.5	-1.5 ± 0.3
LPSHM	47.1	-1.8 ± 0.4

Table 5 Reduced sample-average radii of gyration squared, $\langle R_g^2 \rangle$; asphericity, $\langle A \rangle$; arm radii of gyration squared, $\langle S_{arm}^2 \rangle$; and center to end distance squared, $\langle D_{CTE}^2 \rangle$, computed by molecular simulation for star polymers. The reducing factor is segment diameter, σ; n_{arm} is the number of segments per arm and n is the total number of segments in the polymer molecule.

arms	n_{arm}	n	ε (k_BT)	$\langle R_g^2 \rangle$	$\langle A \rangle$	$\langle S_{arm}^2 \rangle$	$\langle D_{CTE}^2 \rangle$
3	33	100	0	44.0±0.7	0.302±0.006	-	-
3	33	100	-0.15	37.5±0.9	0.292±0.006	-	-
3	33	100	-0.30	30.0±0.5	0.292±0.003	-	-
3	33	100	-0.40	21.0±0.5	0.270±0.002	6.44±0.16	53.7±1.4
3	33	100	-0.50	12.9±0.4	0.203±0.004	5.1±0.2	34±2.5
3	66	199	0	102.0±3.0	0.301±0.004	-	-
3	66	199	-0.15	84.5±2.5	0.294±0.005	21.6±0.4	213±3
3	66	199	-0.30	63.8±0.8	0.294±0.004	17.18±0.25	159.6±2.5
3	66	199	-0.40	37.0±1.4	0.260±0.013	12.05±0.14	94.9±2.6
3	66	199	-0.50	18.8±1.4	0.153±0.017	8.4±0.6	50±4
3	99	298	0	163.5±2.5	0.295±0.005	-	-
3	99	298	-0.15	140.5±1.0	0.295±0.004	35.4±0.7	-
3	99	298	-0.30	99.4±1.6	0.289±0.006	26.5±0.4	-
3	99	298	-0.40	53.9±1.8	0.258±0.005	17.3±0.6	133±6
3	132	397	0	232.0±3.0	0.292±0.004	-	-
4	25	101	0	34.4±0.7	0.210±0.003	-	-
4	25	101	-0.15	30.5±1.5	0.214±0.008	7.59±0.17	69.8±1.9
4	25	101	-0.30	23.8±0.8	0.218±0.007	6.18±0.17	53.8±1.5
4	25	101	-0.40	18.1±0.6	0.215±0.006	5.3±0.17	41.0±1.8
4	25	101	-0.50	12.5±0.2	0.181±0.005	4.31±0.13	28.9±0.7

4	50	201	0	80.5±1.8	0.216±0.004	-	-
4	50	201	-0.15	69.5±1.5	0.221±0.003	15.9±0.5	161±4
4	50	201	-0.30	52.0±1.0	0.223±0.005	13.0±0.2	119±3
4	50	201	-0.40	33.7±1.5	0.222±0.009	9.84±0.25	78.5±2.5
4	50	201	-0.50	18.2±0.9	0.135±0.015	6.9±0.5	38.6±6
4	75	301	0	132.5±2.0	0.220±0.004	-	-
4	75	301	-0.15	112.3±0.8	0.216±0.003	26.3±0.15	258.8±2
4	75	301	-0.30	81.2±1.6	0.228±0.005	20.0±0.5	188±3.5
4	75	301	-0.40	45.4±2.5	0.210±0.007	13.45±0.26	105±3.5
4	100	401	0	185.0±2.5	0.217±0.003	-	-
5	20	101	0	28.0±1.0	0.154±0.003	-	-
5	20	101	-0.15	25.2±0.6	0.162±0.003	6.25±0.06	54.50±0.75
5	20	101	-0.30	20.4±0.2	0.173±0.002	5.40±0.09	44.2±0.7
5	20	101	-0.40	16.0±0.3	0.176±0.002	4.5±0.1	34.3±0.6
5	20	101	-0.50	11.5±0.2	0.156±0.005	3.85±0.08	25.0±0.9
5	40	201	0	66.5±1.5	0.164±0.002	-	-
5	40	201	-0.15	57.5±1.5	0.167±0.004	13.3±0.3	128±3
5	40	201	-0.30	43.4±0.8	0.177±0.007	10.65±0.3	96±3
5	40	201	-0.40	29.8±0.6	0.184±0.003	8.3±0.2	65.8±2.3
5	40	201	-0.50	17.4±0.6	0.130±0.020	6.3±0.3	36.8±2
5	60	301	0	109.0±1.0	0.169±0.002	-	-
5	60	301	-0.15	93.3±1.2	0.169±0.003	20.9±0.3	207±3
5	60	301	-0.30	68.9±0.6	0.178±0.003	16.3±0.15	150.7±1.3
5	60	301	-0.40	42.0±1.5	0.183±0.006	11.5±0.25	91±2
5	80	401	0	154.5±1.5	0.168±0.002	-	-
6	17	103	0	24.8±0.5	0.119±0.002	-	-
6	17	103	-0.15	21.9±0.6	0.125±0.005	5.65±0.18	46.8±1.4
6	17	103	-0.30	18.1±0.3	0.137±0.002	4.84±0.14	37.8±1.0
6	17	103	-0.40	14.5±0.4	0.143±0.005	4.18±0.14	30.1±0.9

6	17	103	-0.50	11.2±0.2	0.133±0.004	3.6±0.1	22.7±0.7
6	34	205	0	57.0±1.5	0.126±0.003	-	-
6	34	205	-0.15	49.5±1.0	0.131±0.003	11.2±0.4	106±2
6	34	205	-0.30	38.9±0.7	0.146±0.003	9.45±0.25	82.6±2
6	34	205	-0.40	27.0±0.6	0.152±0.005	7.35±0.3	57.4±1.9
6	34	205	-0.50	18.4±0.8	0.140±0.015	6.1±0.2	36.5±3
6	51	307	0	94.0±2.0	0.130±0.001	-	-
6	51	307	-0.15	81.2±1.0	0.135±0.002	17.8±0.2	175.5±1.5
6	51	307	-0.30	60.1±1.2	0.148±0.004	14.08±0.25	129±2.5
6	51	307	-0.40	38.4±1.1	0.152±0.006	10.45±0.23	81.6±1.1
6	68	409	0	132.0±1.5	0.131±0.002	-	-

Tab. 6 Estimated asphericity for random-walk star polymers of infinite molecular weight. Data are from Jagodzinski (1994).

Number of arms	Estimated asphericity
3	0.3043
4	0.2427
5	0.2006
6	0.1706

Tab. 7 Reduced osmotic second virial coefficients from molecular simulation as a function of solvent conditions. The reducing parameter is σ^3 where σ is the segment diameter.

Number of arms	Segments per arm	Well depth (k_BT)	B^l_{22} (reduced)
6	17	0	2365±40
6	17	-0.15	1735±25
6	17	-0.30	635±3
6	17	-0.40	-2070±225
6	17	-0.50	-15350±950
6	34	0	7550±80
6	34	-0.15	5680±80
6	34	-0.30	1950±100
6	34	-0.40	-3900±200
6	34	-0.50	-32850±2300

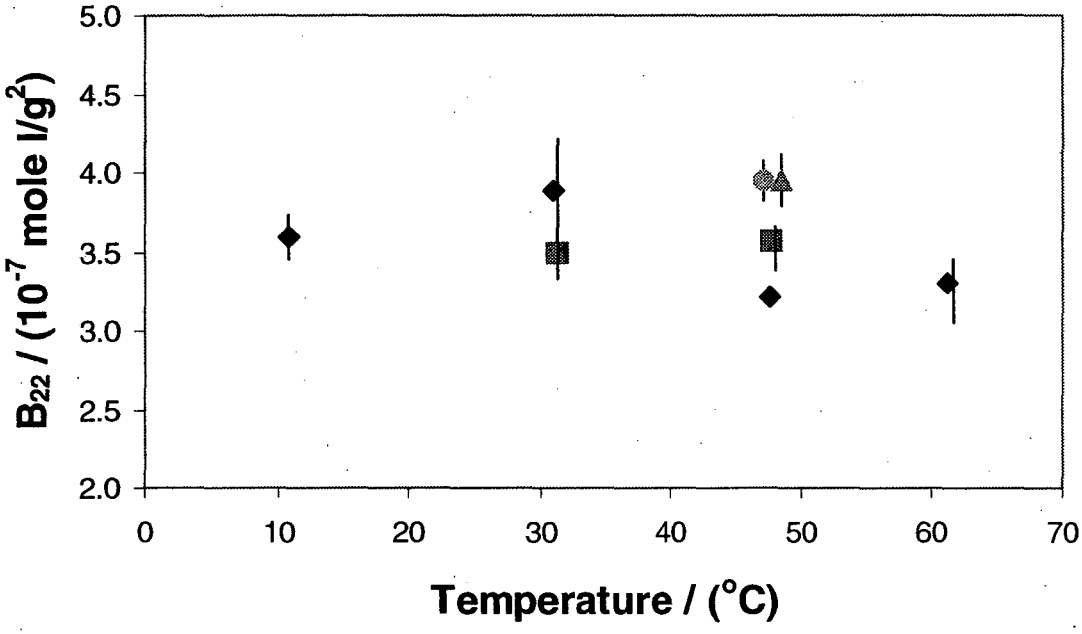

Fig. 1 Osmotic second virial coefficients for different polystyrenes in toluene. Diamonds represent data for SPSLM, squares for SPSHM, triangles for LPSLM, and circles for LPSHM. No significant temperature dependence is observed for SPSLM and SPSHM. Coefficients for star polymers are lower than those for linear polymers.

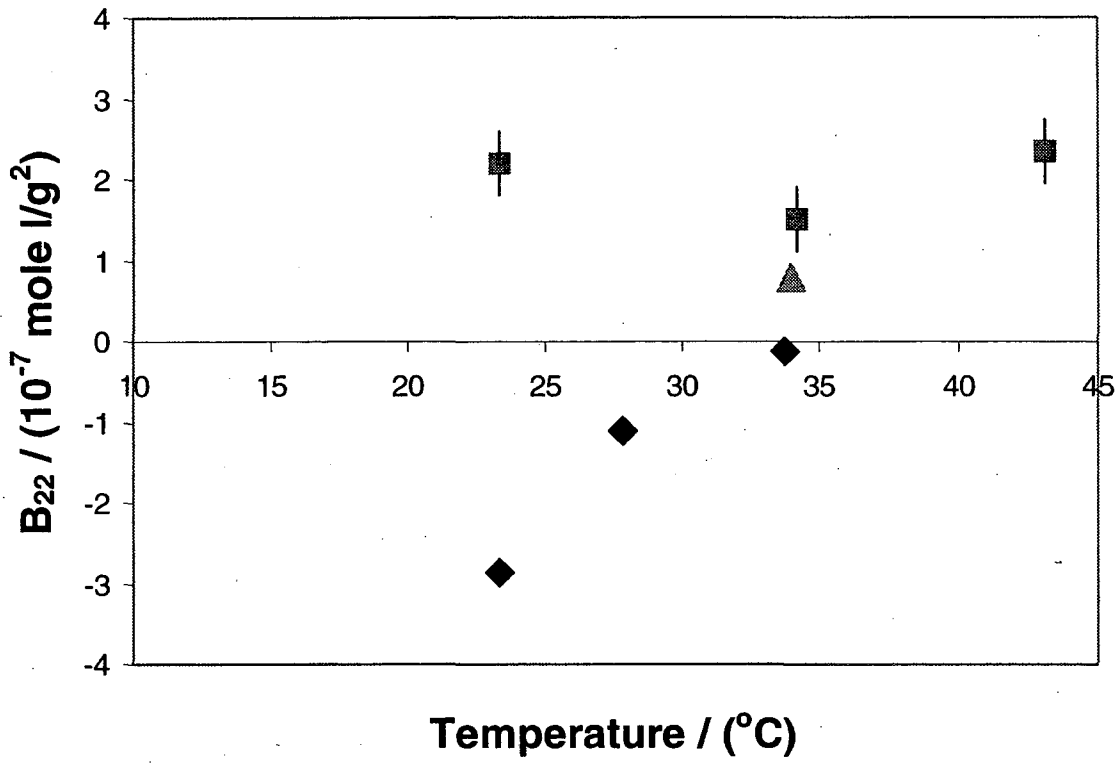

Fig. 2 Osmotic second virial coefficients for different polystyrenes in cyclohexane. Diamonds are for LPSLM, squares for SPSLM, and triangle is for SPSHM. SPSLM presents a theta temperature lower than that for the linear homologue.

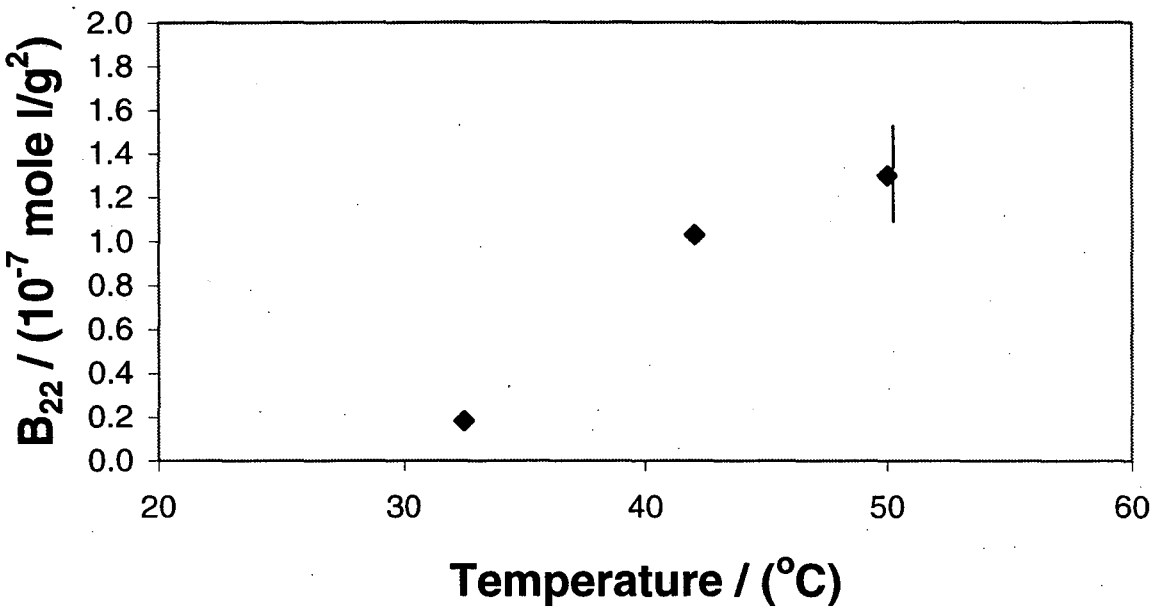

Fig. 3 Osmotic second virial coefficient for SPSLM in methylcyclohexane. Extrapolating the results to $B_{22} = 0$, the theta temperature is 29±3°C.

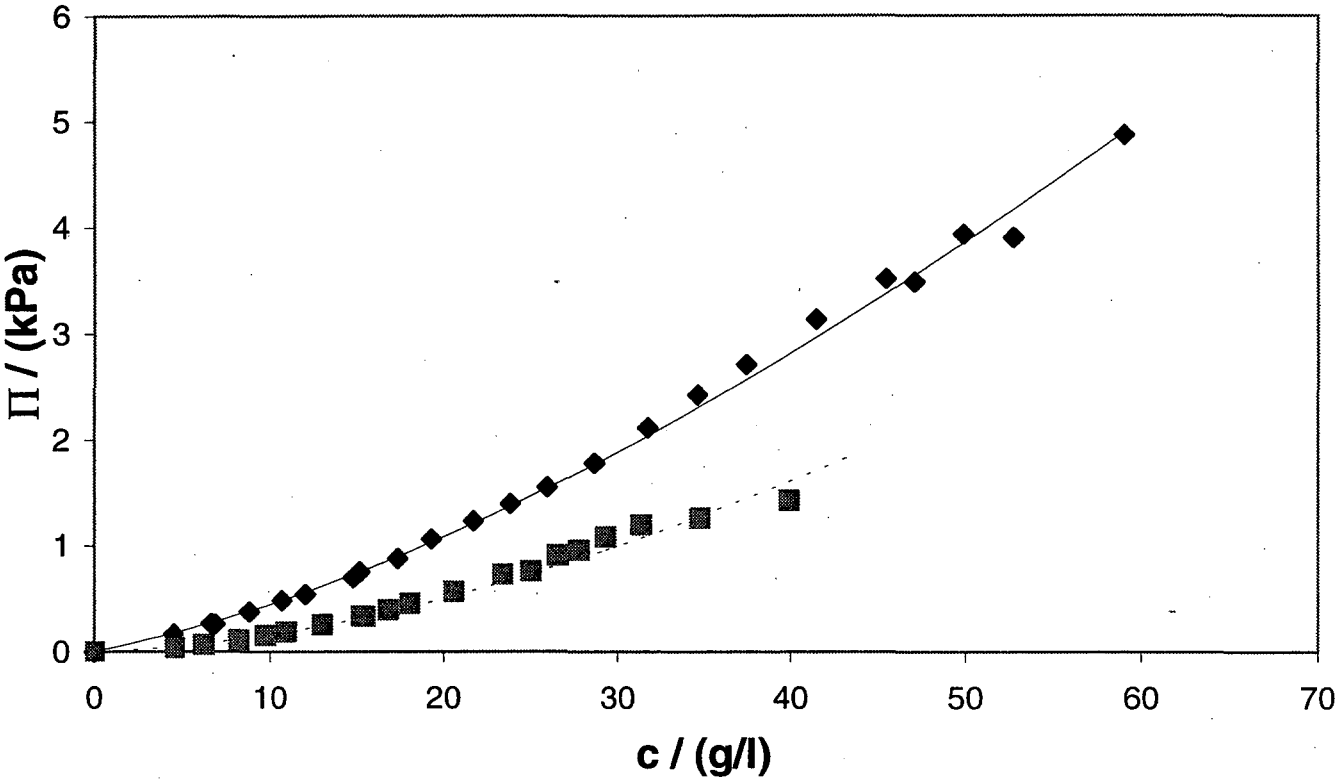

Fig. 4 Osmotic pressure measured for LPSLM and LPSHM in toluene. Diamonds are for LPSLM, squares for LPSHM. Lines are obtained from fitting Equation 1 to the experimental data.

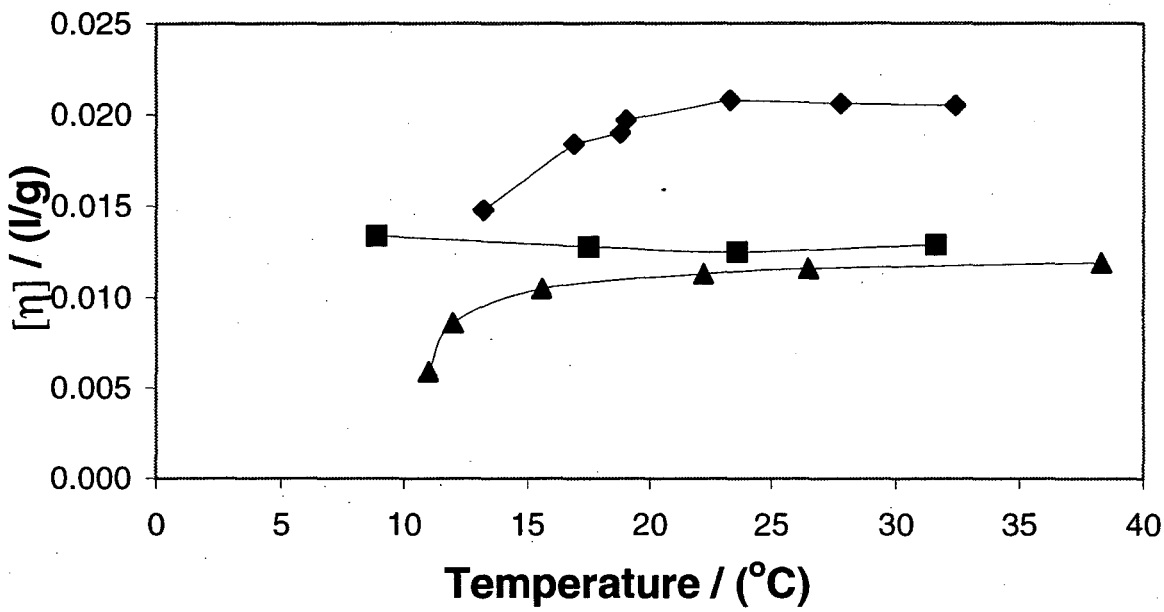

Fig. 5 Intrinsic viscosity for different polystyrenes as a function of temperature. Diamonds represent LPSLM in cyclohexane, squares SPSLM in cyclohexane, and triangles SPSLM in methylcyclohexane. Lines are guides to the eye.

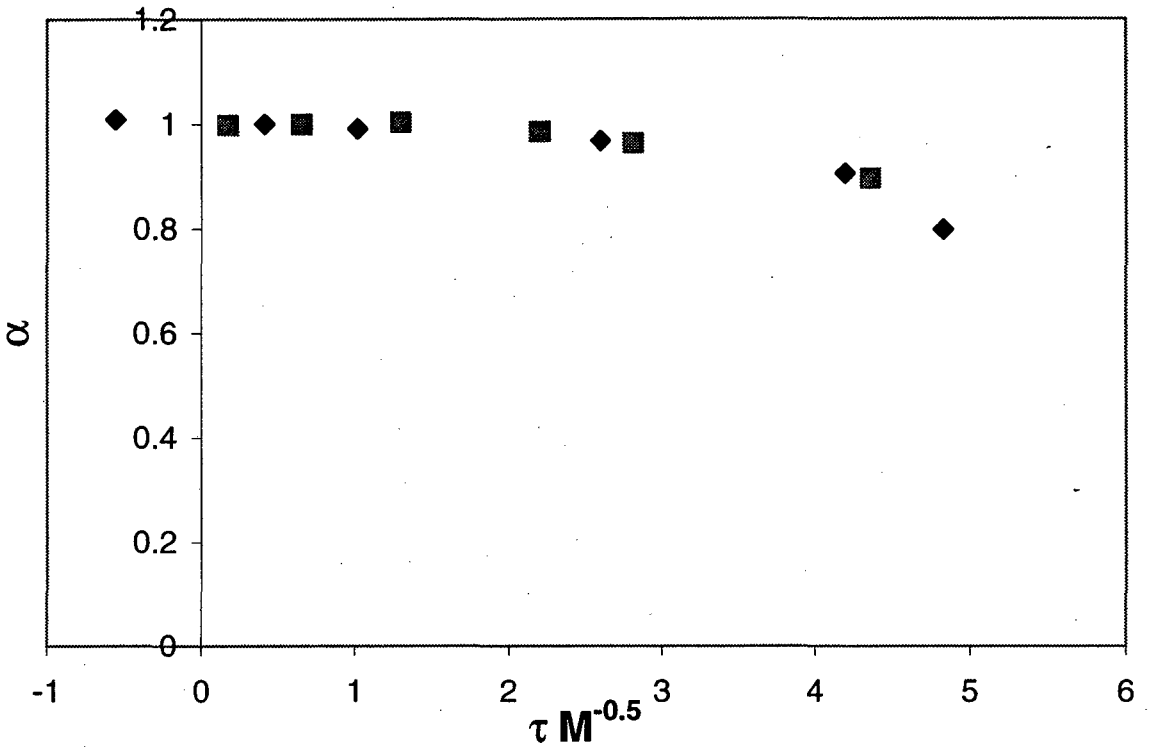

Fig. 6 Expansion factor as a function of reduced temperature times the square root of the polymer molecular weight for LPSLM in cyclohexane (squares) and SPSLM in methylcyclohexane (diamonds). The plot has been obtained assuming a theta temperature 34.5°C for LPSLM in cyclohexane and 30.5°C for SPSLM in methylcyclohexane.

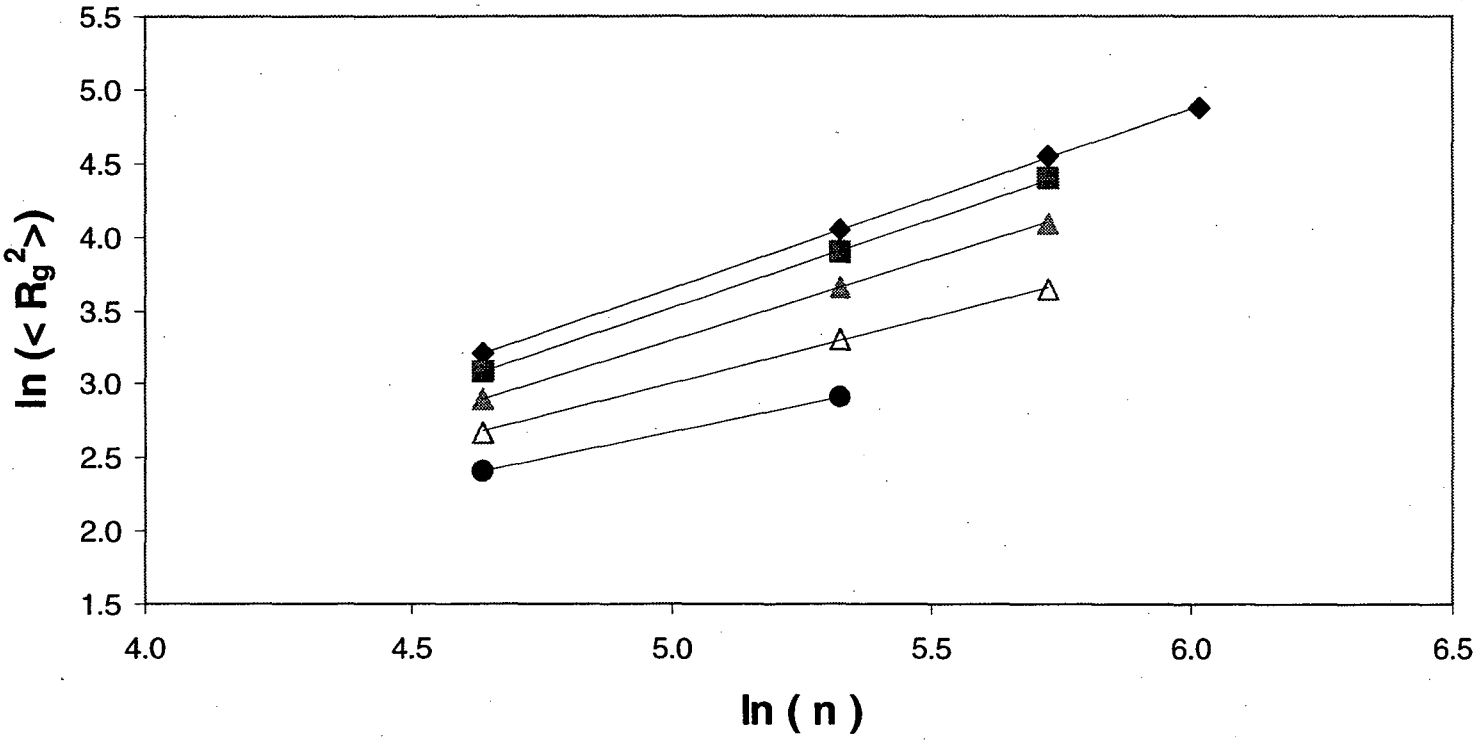

Fig. 7 Radii of gyration squared, $\langle R_g^2 \rangle$, as a function of the number of polymer segments, n, for 6-arm star polymer at different solvent conditions. Diamonds represent athermal conditions, squares well-depth equal to –0.15 k_BT, full triangles –0.30, empty triangles –0.40, and circles –0.50 k_BT.

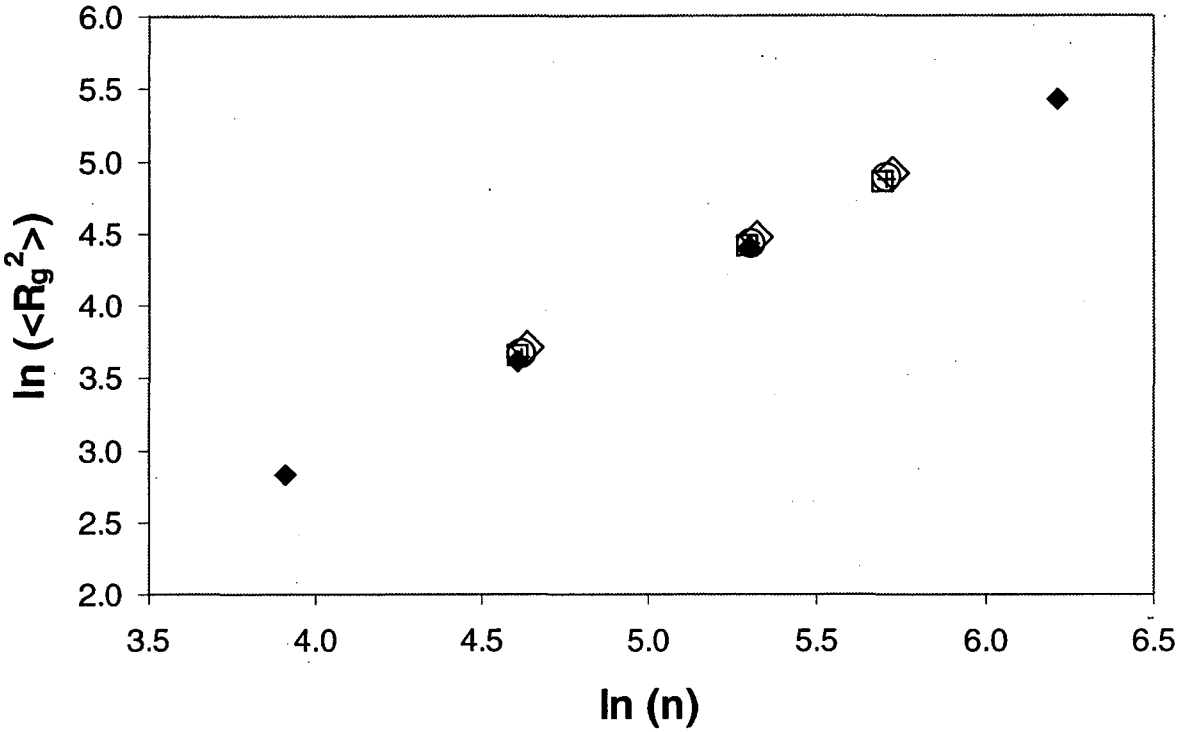

Fig. 8 Radii of gyration as a function of the number of segments for linear polymers at well depth equal to –0.30 k_BT. Full diamonds are data from Dautenhahn and Hall (1994), empty symbols are predicted with Equation14 using the radii of gyration computed for star polymers. Squares represent data computed using results for 3-arm star polymers, crosses for 4-arm, circles for 5-arm, and diamonds for 6-arm star polymers.

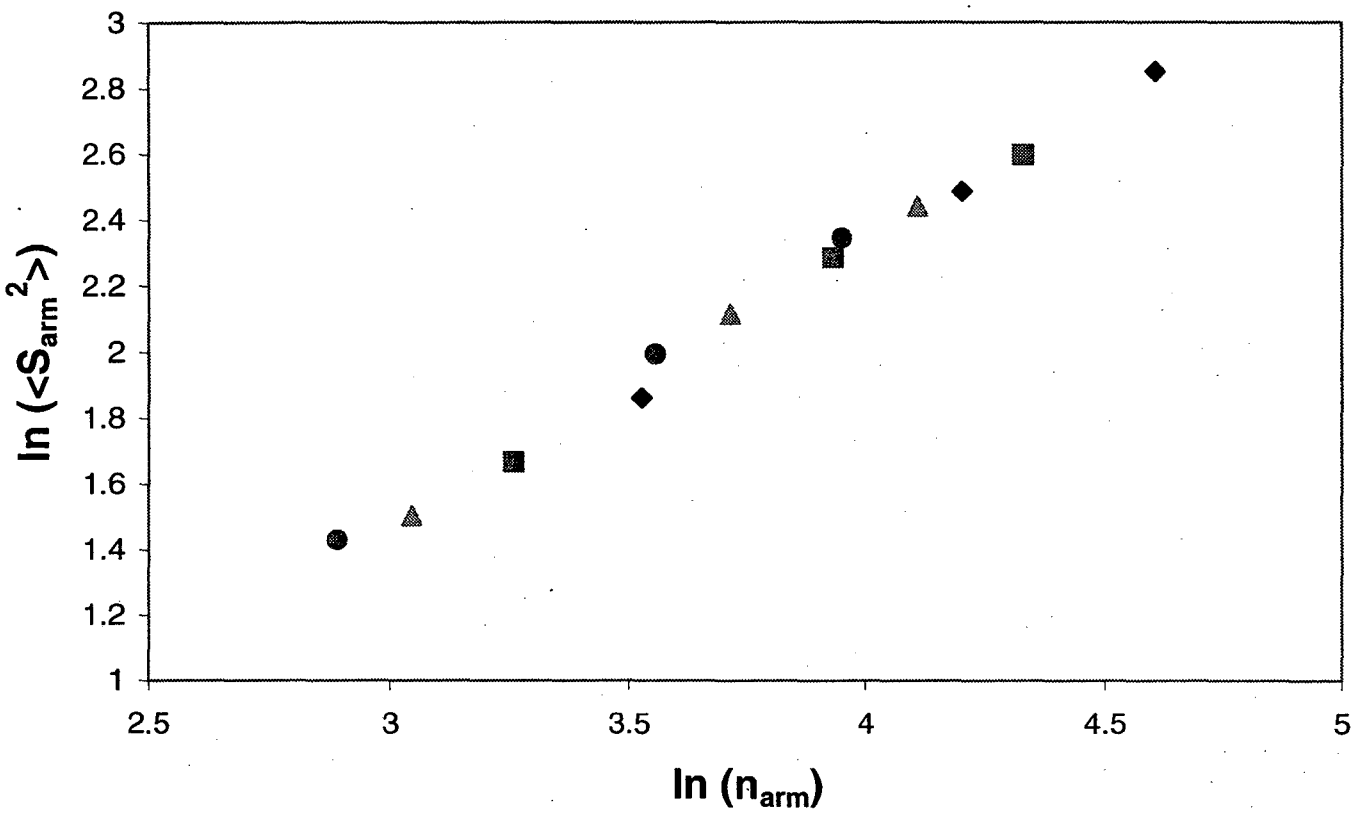

Fig. 9 Arm radius of gyration squared, $<S_{arm}^2>$, as a function of the number of segments in the arm, n_{arm}, for well depth equal to –0.40 k_BT. Diamonds represent results for 3-arm star polymers, squares for 4-arm, triangles for 5-arm, and circles for 6-arm. For equal number of segments in the arm, the arm radius of gyration rises with increasing number of arms, in particular for arms of low molecular weight.

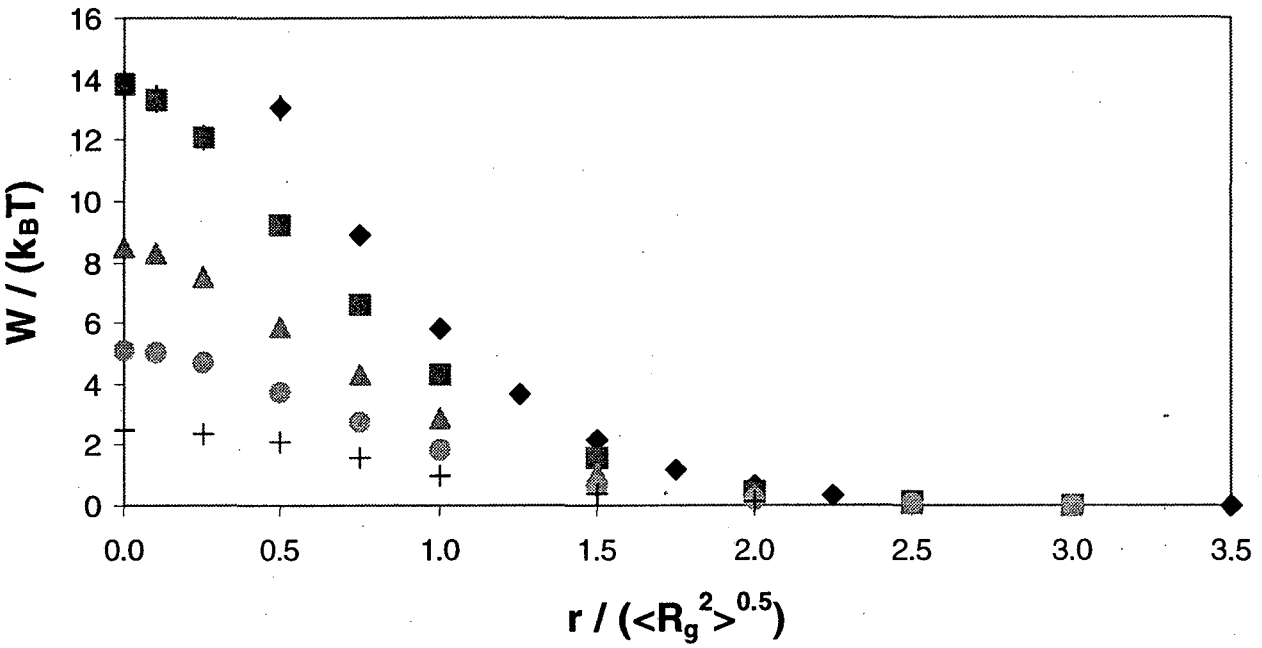

Fig. 10 Potential of mean force as a function of the distance between the centers of mass of the polymers, r, for athermal star polymers of comparable molecular weight but different number of arms; r is normalized by the radius of gyration of the polymer. Circles represent results for 3-arm star, 33 segments per arm; triangles for 4-arm, 25 segments per arm; squares 5-arms, 20 segments per arm; diamonds for 6-arm, 17 segments per arm. Crosses are for linear chains of 100 total segments (Dautenhahn and Hall, 1994). Symbols are larger than the uncertainty.

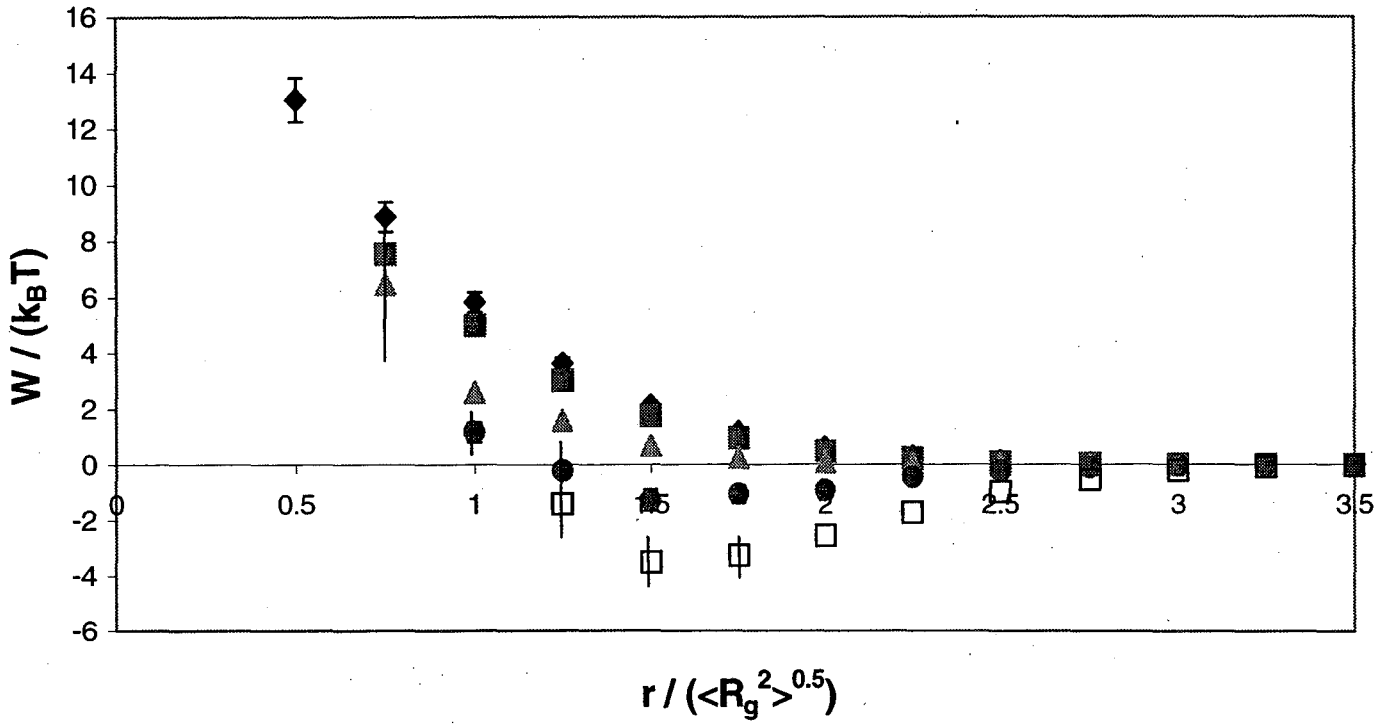

Fig. 11 Potential of mean force as a function of the distance between the centers of mass of the polymers, r, for 6-arm star polymers, 17 segments per arm, at different solvent conditions. Diamonds represent athermal conditions, full squares well-depth equal to –0.15 k_BT, triangles –0.30 k_BT, circles –0.40, and empty squares –0.50 k_BT.

Ernest Orlando Lawrence Berkeley National Laboratory
One Cyclotron Road | Berkeley, California 94720

Prepared for the U.S. Department of Energy under Contract No. DE-AC03-76SF00098